International Journal of Thermophysics, Vol. 9, No. 4, 1988

Temperature Dependence of Thermal Diffusivity Measured by Photothermal Radiometry

D. Gendre,[1] O. Berthet,[1] and M. Huetz-Aubert[1]

Received July 5, 1988

Thermal diffusivity is generally measured by impulse or modulated flux methods; the temperature distribution inside the sample is measured by thermocouples. The nonintrusive photothermal techniques do not induce geometrical or thermal changes inside the sample; an indirect procedure gives the temperature variations on the sample surface. Photothermal radiometry, based on the measurement of the radiative flux emitted by the sample, is all the more accurate as the temperature is elevated. We have used this method to measure thermal diffusivities of thin and opaque solid samples at temperatures above 400 K. The temperature field is calculated by using a standard model accounting for the emitted radiative flux. The experimental apparatus is briefly described and experimental results for selected materials (nickel, stainless steel) and cast-iron samples are presented. The influence of the material structure on the thermal diffusivity is discussed.

KEY WORDS: cast iron; photothermal technique; radiometry; thermal diffusivity.

1. INTRODUCTION

The ability of photothermal technique to detect surface temperature variations in a noncontact manner has made this method of great interest for the measurement of thermal or mechanical properties of materials [1]. A great variety of photothermal techniques, which differ in the probing system, has been applied to thermal diffusivity measurements over the last few years: photoacoustic [1–5], photodeflection [5, 6], mirage effect [5, 7–12], and radiometry [13–16].

[1] Laboratoire d'Energétique Moléculaire et Macroscopique, Combustion, du Centre National de la Recherche Scientifique et de l'Ecole Centrale des Arts et Manufactures, 92295 Châtenay-Malabry Cedex, France.

0195-928X/88/0700-0599$06.00/0

Photothermal radiometry (PTR) uses the detection of thermal radiation emitted by a sample heated by optical means. Cowan [17] and Wheeler [18] had to perform measurements at high temperatures because of the limitation of the detection system they used, which consisted of phototubes. Low-temperature measurements are, nevertheless, possible today due to the development of infrared detectors.

This paper deals with a method for the determination of the thermal diffusivity of thin solid samples above 400 K by photothermal radiometry. The theoretical model is presented in Section 2. The experimental setup is briefly described in Section 3. Experimental results for selected materials (nickel, stainless steel) and some specific cast-iron samples are presented and discussed in Section 4.

2. THEORY

2.1. Presentation of the Model

The model used for the calculation of the temperature distribution is the piston model presented by Rosencwaig and Gersho [2, 19]. Nevertheless, for this application, the thermal radiation emitted by the sample has been taken into account. The bases of this model are the following.

(a) The sample (s) of thickness l_s is front illuminated by electromagnetic radiation, modulated at frequency $f = \omega/2\pi$ (Fig. 1). The

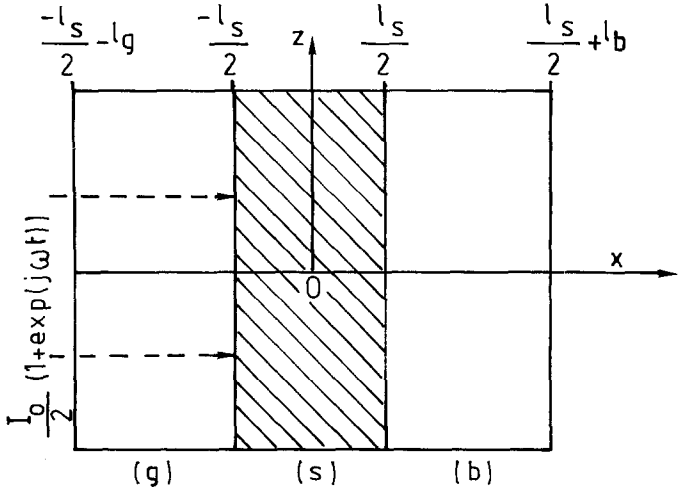

Fig. 1. Schematic diagram of the photothermal cell. g, gas; s, sample; b, back.

geometric distribution of the incident illumination is assumed to be uniform. Its intensity can be written in complex notations as $(I_0/2)(1+e^{j\omega t})$.

(b) The sample is mounted inside a cell. The thermal diffusion length μ_g for the cell is given by

$$\mu_g = \left(\frac{\alpha_g}{\pi f}\right)^{1/2} \tag{1}$$

where α_g is the thermal diffusivity of the gas. μ_g is small when compared with the dimensions of the cell.

(c) The thermal transfer is assumed to be one dimensional in the x direction.

Each variable $\tilde{G}$ of the problem may be considered as the superposition of its continuous $\bar{G}$ and alternative G components:

$$\tilde{G} = \bar{G} + G\exp[j(\omega t + \varphi)] \tag{2}$$

2.2. Solution of the Heat Diffusion Equation for the Open Cell

For the open cell, three regions have to be examined: gas (g), sample (s), and backing (b) (Fig. 1). For these three regions (i = g, s, b), we have

$$\frac{\partial^2 T_i}{\partial x^2} - \frac{j\omega}{\alpha_i} T_i = 0 \tag{3}$$

The corresponding thermal boundary conditions express the continuity of temperature and heat flux, at each interface, and the thermally thick property of the cell:

(a) At $x = -(l_s/2)$,

$$T_s = T_g \tag{4}$$

$$-\lambda_s \frac{\partial T_s}{\partial x} = -\lambda_g \frac{\partial T_g}{\partial x} - 4\bar{\varepsilon}\sigma \bar{T}_s^3 T_s + (1-\rho')\frac{I_0}{2} \tag{5}$$

(b) At $x = l_s/2$,

$$T_s = T_b \tag{6}$$

$$-\lambda_s \frac{\partial T_s}{\partial x} = -\lambda_b \frac{\partial T_b}{\partial x} + 4\bar{\varepsilon}\sigma \bar{T}_s^3 T_s \tag{7}$$

(c) At $x = -(l_s/2) - l_g$,

$$T_g = 0 \tag{8}$$

(d) At $x = (l_s/2) + l_b$,

$$T_b = 0 \tag{9}$$

where λ_i ($i = g, s, b$) is the thermal conductivity of region i and σ is the Stefan–Boltzmann constant.

For the exciting radiation, the material is optically opaque; ρ' is the directional total reflectivity and so $1-\rho'$ is the directional total absorptivity. $\bar{\varepsilon}$ is the hemispherical total emissivity of the sample. The radiative heat flux, exchanged between the sample and the surrounding medium at temperature $\bar{T}_e$, can be expanded to the first order:

$$\tilde{\varphi}_r = \bar{\varepsilon}\sigma[(\bar{T}_s^4 - \bar{T}_e^4) + 4\bar{T}_s^3 T_s \exp[j(\omega t + \varphi)]] \tag{10}$$

The solutions of the heat diffusion Eq. (3) for the three regions are given by

$$-\frac{l_s}{2} - l_g \leqslant x \leqslant -\frac{l_s}{2}, \qquad T_g = D \exp\left[\sigma_g\left(x + \frac{l_s}{2}\right)\right] \tag{11}$$

$$-\frac{l_s}{2} \leqslant x \leqslant \frac{l_s}{2}, \qquad T_s = A \exp\left[-\sigma_s\left(x - \frac{l_s}{2}\right)\right] + B \exp\left[\sigma_s\left(x - \frac{l_s}{2}\right)\right] \tag{12}$$

$$\frac{l_s}{2} \leqslant x \leqslant \frac{l_s}{2} + l_b, \qquad T_b = C \exp\left[-\sigma_s\left(x - \frac{l_s}{2}\right)\right] \tag{13}$$

with

$$C = \frac{(1-\rho')\, I_0}{\lambda_s \sigma_s} \frac{1}{(1+\tau+g)^2\, d^+ - (1-\tau-g)^2\, d^-} \tag{14}$$

$$A = \frac{C}{2}(1+\tau+g) \tag{15}$$

$$B = \frac{C}{2}(1-\tau-g) \tag{16}$$

$$D = \frac{C}{2}[(1+\tau+g)\, d^+ + (1-\tau-g)\, d^-] \tag{17}$$

where

$$\sigma_i = (1+j)\left(\frac{\pi f}{\alpha_i}\right)^{1/2} = \frac{1+j}{\mu_i} \tag{18}$$

$$d^{\pm} = \exp[\pm\sigma_s l_s] \tag{19}$$

$$g = \left[\frac{\lambda_g \rho_g c_g}{\lambda_s \rho_s c_s}\right]^{1/2} \tag{20}$$

$$\tau = \frac{4\bar{\varepsilon}\sigma \bar{T}_s^3}{\lambda_s \sigma_s} = \frac{(1-j)\,M}{\left(\pi \frac{f}{f_c}\right)^{1/2}} \tag{21}$$

with

$$M = \frac{2\bar{\varepsilon}\sigma \bar{T}_s^3 l_s}{\lambda_s} \tag{22}$$

g is the ratio of the thermal effusivities of the gas and sample; for metals this ratio is much smaller than one and can thus be neglected.

2.3. Modulated Radiation Emitted by the Sample

The emitted modulated infrared thermal radiations from the front and rear sides are, respectively,

$$\varphi_r^{fs} = 4\bar{\varepsilon}\sigma \bar{T}_s^3 T_s\left(x = -\frac{l_s}{2}\right) \tag{23}$$

$$\varphi_r^{rs} = 4\bar{\varepsilon}\sigma \bar{T}_s^3 T_s\left(x = \frac{l_s}{2}\right) \tag{24}$$

Substituting T_s in Eqs. (23) and (24) from Eq. (12), we obtain

$$\varphi_r^{fs} = (1-\rho')\, I_0 \left[\frac{\tau}{2}\frac{(1+\tau)\,d^+ + (1-\tau)\,d^-}{(1+\tau)^2 d^+ - (1-\tau)^2 d^-}\right] \tag{25}$$

and

$$\varphi_r^{rs} = (1-\rho')\, I_0 \left[\frac{\tau}{(1+\tau)^2 d^+ - (1-\tau)^2 d^-}\right] \tag{26}$$

Thus, the modulated radiation emitted from the sample on both sides exhibits thermal diffusivity dependence through the terms d^+ and d^- in Eqs. (25) and (26).

The phases of the signal from the front and rear sides are plotted in Figs. 2 and 3, respectively, as a function of $(f/f_c)^{1/2}$, where f_c is the charac-

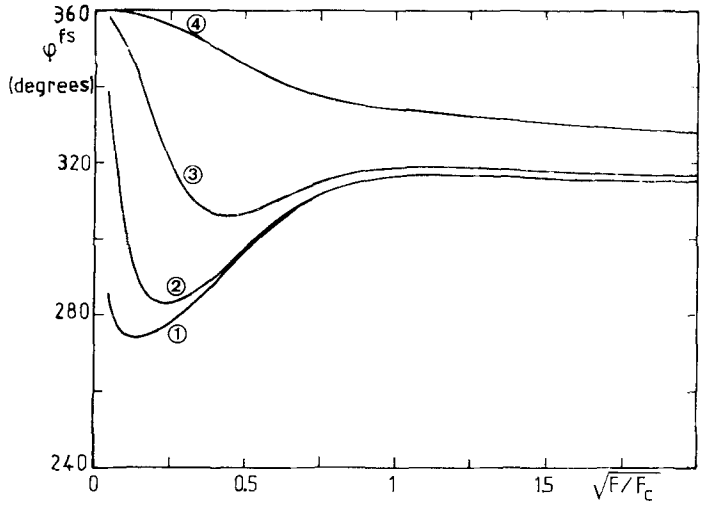

Fig. 2. Phase of the radiation emitted from the front side versus the quantity $(f/f_c)^{1/2}$ for the following values of the parameter M: (1) $M = 10^{-3}$ ($\bar{T}_s \simeq 300$ K); (2) $M = 10^{-2}$ ($\bar{T}_s \simeq 1000$ K); (3) $M = 10^{-1}$ ($\bar{T}_s \simeq 2000$ K); (4) $M = 1$ ($\bar{T}_s \simeq 4500$ K).

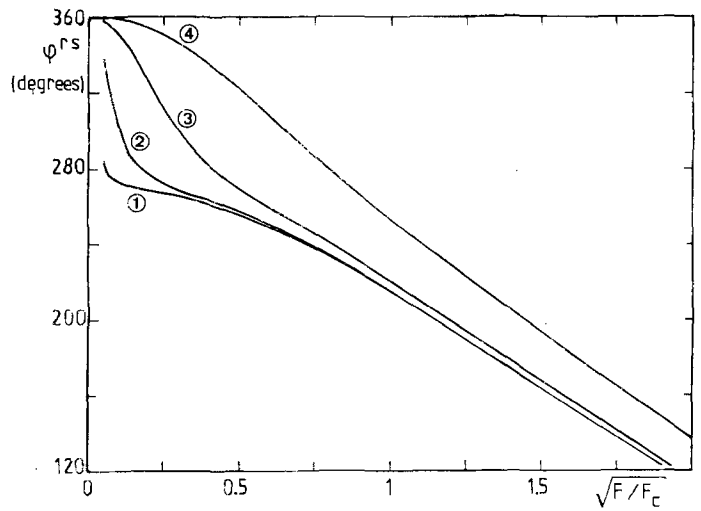

Fig. 3. Phase of the radiation emitted from the rear side versus the quantity $(f/f_c)^{1/2}$ for the following values of the parameter M: (1) $M = 10^{-3}$ ($\bar{T}_s \simeq 300$ K); (2) $M = 10^{-2}$ ($\bar{T}_s \simeq 1000$ K); (3) $M = 10^{-1}$ ($\bar{T}_s \simeq 2000$ K); (4) $M = 1$ ($\bar{T}_s \simeq 4500$ K).

teristic frequency of the sample, $f_c = (\alpha_s/l_s^2)$, and for different values of M, i.e. for different static temperatures.

The following remarks regarding these figures should be noted:

(a) Temperature dependence is more important at low frequencies (thermally thin sample) than at high frequencies (thermally thick sample).

(b) At high frequencies, the phase depends linearly on $(f/f_c)^{1/2}$.

(c) The phase at high frequencies ($f > f_c$) does not depend on M when $M \leqslant 10^{-2}$. Such low values of M are obtained for metals at temperatures below 1000 K.

(d) When $10^{-2} \leqslant M \leqslant 10^{-1}$, the slope of the different phases remains constant, whereas it depends on M for $M > 0.1$: in our case it means temperatures above 2000 K.

Calculations carried out for $M \leqslant 1$ show that the phase of φ_r^{fs} remains equal to $-(\pi/4)$ at high frequencies, whereas, on the rear side, the slope of φ^{rs} is $-\sqrt{\pi}$. It is thus easy to determine f_c, i.e., thermal diffusivity, by recording the phase of the modulated IR radiation emitted by the sample on the rear side for temperatures below 2000 K. Above 2000 K, the term M has to be taken into account.

3. EXPERIMENTAL SETUP

A schematic diagram of the experimental arrangement is shown in Fig. 4. The sample is mounted inside an open cell which can be maintained at a constant temperature $\bar{T}_s$ by an electric heater with a PID regulator.

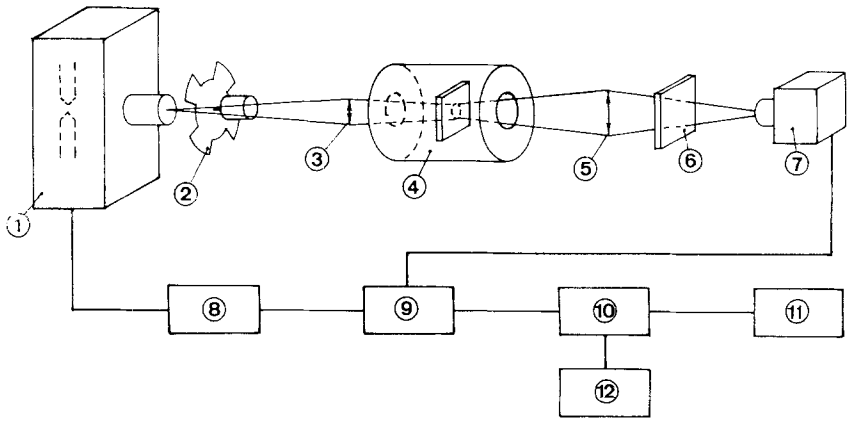

Fig. 4. Experimental setup: (1) Xe lamp; (2) chopper; (3) glass lens L_1; (4) cell + sample; (5) Ca F_2 lens L_2; (6) IR filter; (7) InSb detector; (8) frequency meter; (9) lock-in amplifier; (10) computer; (11) graphics plotter; (12) printer.

The incident radiation, from the arc of a high-pressure Xe lamp, is modulated at different frequencies by a mechanical chopper and focused onto the sample by means of a glass lens L_1.

Thermal radiation emitted from the sample is collected and focused onto the InSb detector by a CaF_2 lens L_2. A band-pass filter, which covers the 3- to 7-μm range, is set in front of the IR detector to remove any optical radiation scattered by the cell from the Xe lamp.

The signal from the InSb detector is processed by a lock-in amplifier (PAR 5204) which gives the phase lag, between the optical radiation (reference) and photothermal signal, for each modulation frequency.

The following remarks should be noted.

(a) The total hemispherical emissivity $\bar{\varepsilon}$ has been introduced in our theoretical model; in fact, $\bar{\varepsilon}$ is the emissivity of the sample surface averaged over the bandwidth of the detection optics and over the solid angle delimited by the aperture of the lens L_2.

(b) In this kind of cell, natural convection is present. This has not perturbed our measurements [22] but it may cause problems at higher temperatures.

(c) In the same way, the sample surface can be oxidized at high temperatures. The results are very different if thin oxide film appears on the sample surface. For this reason, our setup will be modified for operation in a vacuum environment.

Our experimental setup is suitable for measurements above 400 K. Below 400 K, measurements are very uncertain and lead to overestimated values of the thermal diffusivity. However, another experimental setup [22, 23] is available in the laboratory, for measurements of thermal diffusivities by mirage effect, in the 300–500 K range. Experimental results from both methods are compared in the overlaping temperature region.

4. EXPERIMENTAL RESULTS

For each sample, the phase φ^{rs} is measured for about 10 modulation frequencies f greater than f_c. The slope $-\sqrt{\pi/f_c}$ of the line $\varphi^{rs}(\sqrt{f})$ is determined by linear interpolation with a known uncertainty. The resulting relative uncertainty in the thermal diffusivity is 1–2%.

We first tested our experimental system with two usual materials, stainless steel 304 and nickel, whose thermal diffusivities are well known as a function of temperature. Table I lists the experimental results obtained for these two materials and the extremal values reported in the literature [24]. For stainless steel 304, oxidation [25] has limited our measurements up to

800 K. Our results are in good agreement with those reported by other authors. This validates our experimental method.

Several types of cast-iron samples of different structures (ferrite, lower bainite, upper bainite, and perlite) have been studied by the PTR technique. These samples have the same composition and density. The mean diameter of spheroidal graphite is 50 μm. The most important components, expressed as mass percentages, are the following: C, 3.6%; Si, 2.4%; Mn, 0.5%; Cu, 0.5%; S, 0.01%; P, 0.06%; and Mg, 0.03%.

Table II lists the results of the measurements obtained for these samples by mirage effect [22, 23] between 300 and 500 K and by photothermal radiometry. The discrepancy for some values is due to the limits of our experimental devices: the performances of mirage effect above 500 K and of photothermal radiometry below 400 K are reduced. Furthermore, oxidation perturbs measurements at high temperatures.

Figure 5 shows the variation of the thermal diffusivity for different structures of cast iron as a function of temperature. These plots are linear above 500 K and the slopes of these plots vanish, except for ferrite. The values of thermal diffusivity are a characteristic of each structure, except for upper bainite, for which the plot tends rapidly to be similar to that of the lower bainite above 500 K. A microphotographic analysis of the upper

Table I. Comparison Between the Present Results and Those of Other Authors [24]

Sample (thickness)	Temperature (K)	Thermal diffusivity $\times 10^5 (m^2 \cdot s^{-1})$		
		Present results	Reported in Ref. 24	
			Max.	Min.
Stainless steel (300 μm)	500	0.35 ± 0.13	0.44	0.35
	600	0.38 ± 0.07	0.46	0.37
	700	0.43 ± 0.09	0.48	0.37
	800	0.44 ± 0.09	0.50	0.40
Nickel (520 μm)	500	1.44 ± 0.04	1.60	1.20
	600	1.00 ± 0.01	1.40	1.10
	700	1.20 ± 0.01	1.45	1.15
	800	1.33 ± 0.02	1.60	1.25
	900	1.30 ± 0.01	1.50	1.30
	1000	1.33 ± 0.02	1.50	1.25
	1050	1.37 ± 0.02	1.50	1.28

bainite sample, after the experiments, has shown that the structure of this material had been modified [22]. These experiments point out the great sensitivity of the thermal diffusivity to any modification of the structure and confirm the results of similar studies [26–28].

Table II. Experimental Results for Cast-Iron Samples: (1) From Mirage Effect in the 300–500 K Range; (2) From Photothermal Radiometry in the 400–800 K Range

Sample	Temperature (K)	Thermal diffusivity $\times 10^6$ ($m^2 \cdot s^{-1}$)
Upper bainite	320	10.60 (1)
	370	8.65 (1)
	400	7.92 (1)
		7.44 (2)
	500	6.28 (1)
		5.90 (2)
	600	5.90 (2)
	700	6.51 (2)
	800	5.73 (2)
Lower bainite	320	8.01 (1)
	360	7.29 (1)
	400	6.50 (1)
		7.33 (2)
	500	6.42 (1)
		6.01 (2)
	600	5.96 (2)
	700	5.87 (2)
	800	5.29 (2)
Perlite	330	8.65 (1)
	350	7.45 (1)
	400	7.29 (1)
		6.27 (2)
	500	6.79 (1)
		5.71 (2)
	600	5.53 (2)
	700	5.65 (2)
	800	6.33 (2)
Ferrite	330	10.04 (1)
	400	8.88 (1)
		13.73 (2)
	500	7.49 (1)
		8.60 (2)
	600	8.15 (2)
	700	7.63 (2)

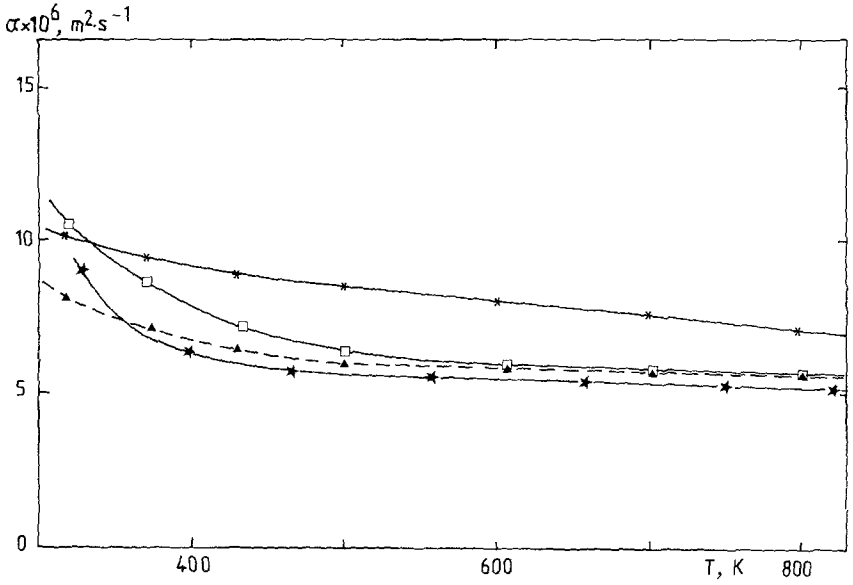

Fig. 5. Thermal diffusivity vs temperature for cast-iron samples. (□) Upper bainite; (▲) lower bainite; (★) perlite; (*) ferrite.

5. CONCLUSION

Photothermal radiometry is an accurate technique for measurements of thermal diffusivity at high temperatures. However, it is necessary to use a vacuum chamber in order to reduce oxidation and increase the temperatures to above 800 K. The experimental results obtained for nickel and stainless steel 304 are in good agreement with those reported in the literature. Besides, the measurements by photothermal radiometry are in good agreement with the values obtained by mirage effect. The experimental results for cast-iron samples show the great dependence of thermal diffusivity on the material structure.

ACKNOWLEDGMENT

The authors wish to thank the Saint Gobain-Pont à Mousson Company which has, in part, supported this work.

REFERENCES

1. Topical Meetings on Photoacoustic and Photothermal Spectroscopy, OSA, Ames, Aug. 1979; OSA, Berkeley, June 1981; CNRS-ESPCI, Paris, Apr. 1983; Ecole Polytechnique, Montreal, Aug. 1985.
2. A. Rosencwaig, *Photoacoustics and Photoacoustic Spectroscopy*, Wiley, New York (1980).
3. F. A. Mac Donald and G. C. Wetsel, Jr., *J. Appl. Phys.* **49**:2313 (1978).
4. W. Jackson and N. M. Amer, *J. Appl. Phys.* **51**:3343 (1980).
5. G. Rousset, Thèse de Docteur-Ingénieur (Ecole Centrale de Paris, Paris, 1983).
6. G. Rousset, F. Lepoutre, and L. Bertrand, *J. Appl. Phys.* **54**:2383 (1983).
7. L. C. Aamodt and J. C. Murphy, *J. Appl. Phys.* **51**:1580 (1980).
8. L. C. Aamodt and J. C. Murphy, *J. Appl. Phys.* **52**:4903 (1981).
9. W. B. Jackson, N. M. Amer, A. C. Boccara, and D. Fournier, *Appl. Optics* **20**:1333 (1981).
10. J. C. Murphy and L. C. Aamodt, *J. Appl. Phys.* **51**:4580 (1980).
11. G. Rousset and F. Lepoutre, *Rev. Phys. Appl.* **17**:201 (1982).
12. K. R. Grice, L. J. Inglehart, L. D. Favro, P. K. Kuo, and R. L. Thomas, *J. Appl. Phys.* **54**:6245 (1983).
13. P. E. Nordal and S. O. Kanstad, *Infrared Phys.* **25**:295 (1985).
14. A. C. Tam, *Infrared Phys.* **25**:305 (1985).
15. G. Busse, *Appl. Optics* **21**:107 (1982).
16. W. P. Leung and A. C. Tam, *J. Appl. Phys.* **56**:153 (1985).
17. R. D. Cowan, *J. Appl. Phys.* **32**:1363 (1961).
18. M. J. Wheeler, *Br. J. Appl. Phys.* **16**:365 (1965).
19. A. Rosencwaig and A. Gersho, *J. Appl. Phys.* **47**:64 (1976).
20. P. Cielo, *J. Appl. Phys.* **56**:230 (1985).
21. W. D. Lawson and J. W. Sabey, in *Research Techniques in N.D.T.*, R. S. Sharpe, ed. (Academic, London, 1970), Chap. 4.
22. D. Gendre, Thèse de Docteur Ingénieur (Ecole Centrale de Paris, 1986).
23. D. Gendre, *Rev. Gen. Therm.* **26**:54 (1987).
24. Y. S. Touloukian, R. W. Powel, C. Y. Ho, and M. C. Nicolao, *Thermal Diffusivity* (I.F.I. Plenum, New York, 1973), Vol. 10.
25. J. M. Ané and M. Huetz-Aubert, *Int. J. Thermophys.* 7:1191 (1986).
26. A. Degiovanni, A. M. Gery, M. Laurent, and G. Sinicki, *Mem. Sci. Rev. Metal.* Feb. (1977).
27. Y. Tanaka, H. Saito, I. Tokura, and K. Ikawa, *Trans. ASME* **104**:61 (1982).
28. J. Ormerod, R. Taylor, and R. Edwards, *Metals Technol.* **5**:109 (1978).